Hindawi
Contrast Media & Molecular Imaging
Volume 2017, Article ID 6162845, 7 pages
https://doi.org/10.1155/2017/6162845

Clinical Study

A First Report on [^{18}F]FPRGD$_2$ PET/CT Imaging in Multiple Myeloma

Nadia Withofs,[1] François Cousin,[1] Bernard De Prijck,[2] Christophe Bonnet,[2] Roland Hustinx,[1] Sanjiv S. Gambhir,[3] Yves Beguin,[2] and Jo Caers[2]

[1]*CHU of Liege, Nuclear Medicine and Oncological Imaging Division, Medical Physics Department, Liege, Belgium*
[2]*CHU of Liege, Department of Clinical Hematology, Liege, Belgium*
[3]*Molecular Imaging Program at Stanford (MIPS), Radiology Department, Stanford University, Stanford, CA, USA*

Correspondence should be addressed to Jo Caers; jo.caers@chu.ulg.ac.be

Received 19 March 2017; Revised 15 May 2017; Accepted 13 June 2017; Published 27 July 2017

Academic Editor: Xuelei Ma

An observational study was set up to assess the feasibility of [^{18}F]FPRGD$_2$ PET/CT for imaging patients with multiple myeloma (MM) and to compare its detection rate with low dose CT alone and combined [^{18}F]NaF/[^{18}F]FDG PET/CT images. Four patients (2 newly diagnosed patients and 2 with relapsed MM) were included and underwent whole-body PET/CT after injection of [^{18}F]FPRGD$_2$. The obtained images were compared with results of low dose CT and already available results of a combined [^{18}F]NaF/[^{18}F]FDG PET/CT. In total, 81 focal lesions (FLs) were detected with PET/CT and an underlying bone destruction or fracture was seen in 72 (89%) or 8 (10%) FLs, respectively. Fewer FLs (54%) were detected by [^{18}F]FPRGD$_2$ PET/CT compared to low dose CT (98%) or [^{18}F]NaF/[^{18}F]FDG PET/CT (70%) and all FLs detected with [^{18}F]FPRGD$_2$ PET were associated with an underlying bone lesion. In one newly diagnosed patient, more [^{18}F]FPRGD$_2$ positive lesions were seen than [^{18}F]NaF/[^{18}F]FDG positive lesions. This study suggests that [^{18}F]FPRGD$_2$ PET/CT might be less useful for the detection of myeloma lesions in patients with advanced disease as all FLs with [^{18}F]FPRGD$_2$ uptake were already detected with CT alone.

1. Background

The introduction of efficient and less toxic treatments caused a paradigm shift in the management of multiple myeloma (MM) towards an earlier diagnosis and treatment [1, 2]. To detect early signs of bone disease and to identify those patients for whom treatment is needed, highly sensitive imaging techniques are required. Positron emission tomography combined with computed tomography (PET/CT) using [^{18}F]fluorodeoxyglucose ([^{18}F]FDG) has already proven to be a sensitive technique for the detection of metabolically active MM lesions and was recently incorporated in the diagnostic work-up of MM by the International Myeloma Working Group (IMWG) accordingly [3].

Alternatively, the ^{18}F-FB-mini-PEG-E[c(RGDyK)]$_2$ ([^{18}F]FPRGD$_2$), a validated radiopharmaceutical with high binding affinity for integrin $\alpha_v\beta_3$, seems attractive for the detection of MM lesions [4–8]. The RGD-based radiopharmaceuticals were initially developed to accelerate the development of therapies targeting integrin $\alpha_v\beta_3$ [9]. The high expression of integrin $\alpha_v\beta_3$ by activated endothelial cells during angiogenesis aroused keen interest in RGD-based radiopharmaceuticals for imaging of tumor angiogenesis [10, 11]. Nevertheless, the integrin $\alpha_v\beta_3$ is not solely expressed by activated endothelial cells; it can be overexpressed by many types of cancer cells, regulating cell survival, metastases, and drug resistance [12]. In the case of myeloma, the integrin $\alpha_v\beta_3$ is expressed by activated endothelial cells but it can also be overexpressed by myeloma tumor cells and other cell types of the tumor microenvironment such as osteoclasts [13–17]. Our group previously studied the use of [^{18}F]FPRGD$_2$ in rectal and renal cancers, where a correlation between integrin $\alpha_v\beta_3$ expression and tracer uptake was shown [7, 8]. Since multiple players within the myeloma microenvironment express the integrin $\alpha_v\beta_3$, we hypothesized that [^{18}F]FPRGD$_2$ PET/CT could be an

effective imaging technique for the detection of myeloma lesions.

The combination of [^{18}F]NaF and [^{18}F]FDG for PET/CT is another strategy to improve the detection of bone metastases and was first introduced by Iagaru et al. [18, 19]. The rationale for the use of both [^{18}F]NaF, allowing the detection of bone metastases with bone formation, and [^{18}F]FDG, enabling the detection of metastases with increased rate of glucose metabolism, was to improve the sensitivity for detecting metastatic lesions. A prospective clinical trial evaluating combined [^{18}F]NaF and [^{18}F]FDG for PET/CT in patients with MM is currently under investigation (EudraCT 2013-004807-38), aiming at comparing its capacity to detect MM lesions with the capacities of magnetic resonance imaging, CT alone, and whole-body X-rays [20].

The current observational study was set up to assess the feasibility of [^{18}F]FPRGD$_2$ PET/CT to identify myeloma lesions. Secondarily, the detection rate of [^{18}F]FPRGD$_2$ PET/CT was compared to CT alone. Additionally, [^{18}F]FPRGD$_2$ PET/CT images were compared to combined [^{18}F]NaF/[^{18}F]FDG PET/CT images, available for those patients that were also included in the above-mentioned trial [20].

2. Materials and Methods

Patients with newly diagnosed or relapsed MM were prospectively included. This study was registered as EudraCT #2013-004807-38 and was approved by the Ethics Committee of the academic hospital (CHU of Liege). All subjects provided written informed consent for this study.

The radiosynthesis of [^{18}F]FPRGD$_2$ was performed as previously reported and in compliance with current good manufacturing practice regulations [5, 7]. The mean (±standard deviation) injected mass of the active pharmaceutical ingredient was 11.1 μg (±1.6 μg) [7].

Every patient underwent whole-body (WB) scans, from vertex to toes, using [^{18}F]FPRGD$_2$ PET/CT and combined [^{18}F]NaF/[^{18}F]FDG PET/CT (median delay between scans: 4 days; range: 3–5 d). PET/CT scans were acquired in a Gemini TF scanner after injection of 296 ± 9 MBq [^{18}F]FPRGD$_2$ (median uptake time: 62 min) or 133 ± 6 MBq [^{18}F]NaF and 242 ± 27 MBq [^{18}F]FDG (median delay between [^{18}F]FDG and [^{18}F]NaF injections: 2 min and uptake time: 66 min). All patients fasted for 6 h prior to radiopharmaceutical injection (glycemia < 120 μg/ml in all patients). A low dose CT (3 mm slice thickness; 120 kV and 50 to 80 mAs depending on patient's weight) followed by the PET emission scan of 90 seconds per bed position was performed.

The PET/CT images were reviewed by 2 experienced nuclear medicine physicians and 2 radiologists to detect focal lesions (FLs) and/or diffuse bone marrow involvement. Areas of tracers' uptake corresponding to degenerative changes were excluded. Focal areas of increased uptake, regardless of the presence of bone abnormality on CT images, and hypoactive FLs with underlying bone destruction on CT images and suspected of being associated with myeloma lesions were considered PET MM FLs. The FLs were classified according to their location in 7 regions of the body: pelvis, skull, superior limbs, inferior limbs, spine, ribs, and one location including the sternum, scapula, and clavicles. A 1.2 ml volume of interest was drawn in the focal area of radiopharmaceutical's uptake to estimate the maximum standardized uptake value (SUV_{max}). The maximum diameter of the osteolytic lesions, when present, was also measured. The results are presented as means ± standard deviation (SD).

Table 1: Patients' characteristics (n = 4).

Feature	n
Median age (range)	
65 (51–79) years	4
Sex	
Female	1
Male	3
Mean ± SD BMPC infiltration (%)	
48 ± 29%	4
Ig isotype	
IgG	4
ISS stage at diagnosis	
I	1
III	3
Relapsed MM	
Time from diagnosis	
40 & 58 months	2
Time from last treatment	
35 & 52 months	
Prior treatment	
Thalidomide-dexamethasone/ASCT	1
Melphalan-prednisone-thalidomide	1
No prior bisphosphonates therapy	4

Ig = immunoglobulin; BMPC = bone marrow plasma cell; ASCT = autologous stem cell transplantation.

3. Results

Four patients with MM were included, n = 2 with newly diagnosed MM and n = 2 with relapsed MM (Table 1). Based on the low dose CT images, the pattern of bone marrow involvement was focal (n = 2) or combined diffuse and focal (n = 2). Per patient, ≤3 FL (n = 2) or >10 FLs (n = 2) were detected. No extramedullary disease was detected. Overall, 81 FLs were detected with PET/CT with underlying bone destruction on CT images (n = 72; 89%) or fractures (n = 8; 10%; vertebra n = 5; rib n = 3) and one FL (1%) detected with [^{18}F]NaF/[^{18}F]FDG PET in the femur did not show any abnormality on CT images. Overall, the detection rate of [^{18}F]FPRGD$_2$ PET was lower than [^{18}F]NaF/[^{18}F]FDG PET, whatever the FL location, and the mean uptake (SUV_{max}) of [^{18}F]FPRGD$_2$ was overall lower than [^{18}F]NaF/[^{18}F]FDG (Table 2). Out of the 72 osteolytic FLs detected with the CT of the PET, only 50% (36/72) showed [^{18}F]FPRGD$_2$ uptake (Figure 1). Nonetheless, in one patient with newly diagnosed MM (Figure 1: patient #1), five

Table 2: Focal lesions detected with CT and PET and lesions' characteristics.

	Whole-body CT	$[^{18}F]FPRGD_2$ PET	$[^{18}F]NaF/[^{18}F]FDG$ PET
Number of osteolytic lesions ($n = 72$)	$n = 72$ (89%)	$n = 36$ (44%)	$n = 47$ (64%)††
Mean ± SD SUV_{max}		*2.5 ± 0.8*	*8.5 ± 4.3*
Number of fractures ($n = 8$)	$n = 8$ (10%)	$n = 8$ (10%)	$n = 8$ (10%)
Mean ± SD SUV_{max}		*3.3 ± 1.2*	*9.4 ± 2.3*
Number of FLs without any abnormality on CT images	$n = 0$	$n = 0$	$n = 1$ (1%)
Total number of FLs ($n = 81$)†	$n = 80$ (99%)	$n = 44$ (54%)	$n = 56$ (69%)

†Number of FLs regardless of the presence of bone abnormality on low dose CT images, or hypoactive FLs with underlying bone destruction on CT images were considered PET FLs. ††Two out of 47 were hypoactive FLs; they were not considered in the measurement of SUV.

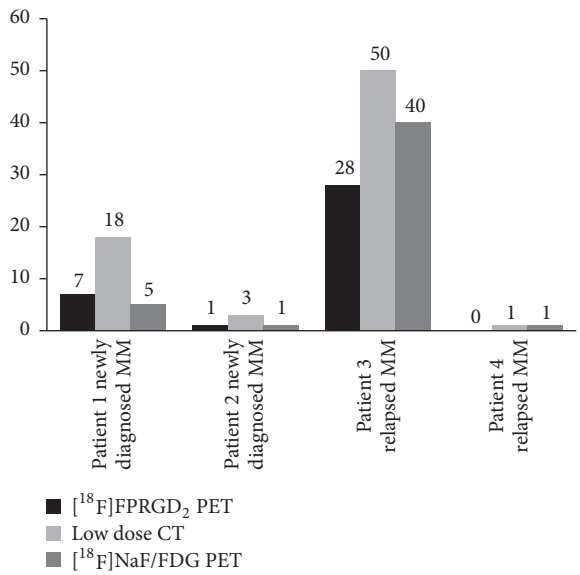

Figure 1: Detection rate of osteolytic FLs of CT, $[^{18}F]NaF/FDG$ PET/CT, and $[^{18}F]FPRGD_2$ PET/CT per patient ($n = 4$) and overall.

FLs showed $[^{18}F]FPRGD_2$ uptake but no $[^{18}F]NaF/[^{18}F]FDG$ uptake (Figure 2). In patient # 2 (Figure 1), both $[^{18}F]FPRGD_2$ and $[^{18}F]NaF/[^{18}F]FDG$ PET/CT detected one rib osteolytic FL, while 2 additional osteolytic FLs were detected with CT. In patient #3 (Figure 1), the detection rate of $[^{18}F]FPRGD_2$ PET was much lower than $[^{18}F]NaF/[^{18}F]FDG$ PET (Figure 3). In patient #4 (Figure 1), $[^{18}F]FPRGD_2$ PET/CT overlooked one 5 mm osteolytic FL of the cortical bone of a femur that was detected with $[^{18}F]NaF/[^{18}F]FDG$ PET/CT. In the contingency Table 3, the obtained results in patients with newly diagnosed disease are compared to those of patients with relapsing disease. $[^{18}F]FPRGD_2$ positive lesions without concomitant $[^{18}F]NaF/[^{18}F]FDG$ uptake were observed in one patient with newly diagnosed disease, while patient #3 (with a disease relapse) showed $[^{18}F]NaF/[^{18}F]FDG$ positive lesions without $[^{18}F]FPRGD_2$ uptake.

4. Discussion

Our purpose was to explore the detection capabilities of $[^{18}F]FPRGD_2$ PET/CT and to assess its feasibility in MM disease. In the studied patients, the detection rate of $[^{18}F]FPRGD_2$ PET was lower than the detection rate of low dose CT alone (Figure 1). Every FL showing $[^{18}F]FPRGD_2$ uptake corresponded to an osteolytic lesion or a fracture on low dose CT images. Although the integrin $\alpha_v\beta_3$ is expressed by multiple cells in tumor microenvironment such as MM tumor cells, osteoclasts, and activated endothelial cells during angiogenesis, our clinical observation suggests that $[^{18}F]FPRGD_2$ PET/CT does not allow a higher detection rate of MM bone lesions than low dose CT alone. The detection rate of $[^{18}F]FPRGD_2$ PET was overall lower than $[^{18}F]NaF/[^{18}F]FDG$ PET (patient #3; Figures 1 and 3) but in one patient, more lesions were visible on the $[^{18}F]FPRGD_2$ scan (patient #1; Figures 1 and 2). The prognostic value of $[^{18}F]FPRGD_2$ positive lesions and the value of $[^{18}F]FPRGD_2$ PET/CT in patients with asymptomatic disease (and thus without bone lesions) were not studied and could be of interest. On the other hand, the high bone marrow background activity related to $[^{18}F]NaF$ uptake may explain why some of the FLs detected with $[^{18}F]FPRGD_2$ PET/CT were not seen with $[^{18}F]NaF/[^{18}F]FDG$. Diffuse bone marrow infiltration was not reliably estimated with $[^{18}F]NaF/[^{18}F]FDG$ PET due to high $[^{18}F]NaF$ bone uptake while it was suspected with $[^{18}F]FPRGD_2$ PET/CT in 2 of the 4 patients (Figure 4).

Our report included 2 patients with relapsed MM and thus with possible long-lasting healed lesions. In one of these patients (patient #3; Figure 3), some of the osteolytic lesions did not show uptake of $[^{18}F]FPRGD_2$ while $[^{18}F]NaF/[^{18}F]FDG$ PET showed tracer's uptake in all these lesions, indicating residual activity. However, whether the uptake was related to $[^{18}F]FDG$ in the presence of residual metabolically active tumor and/or whether it was related to $[^{18}F]NaF$ due to bone turnover in the long-lasting healing process of bone lesions after treatment is unknown [21]. Moreover, we excluded patients with a short treatment-free interval before inclusion to avoid PET-negativity induced by a recent chemotherapy.

As mentioned in the introduction, both imaging techniques highlight different biological aspects. $[^{18}F]FPRGD_2$ allows the estimation of integrin $\alpha_v\beta_3$ expression by endothelial cells (and thus neovascularization), tumor cells, and activated osteoclasts, while $[^{18}F]NaF/[^{18}F]FDG$ uptake reflects

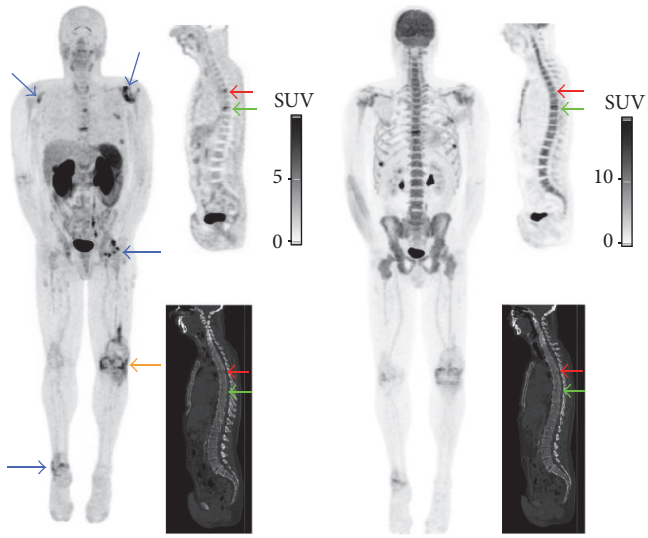

Figure 2: [^{18}F]FPRGD$_2$ and [^{18}F]NaF/[^{18}F]FDG PET/CT images of patient #1 with newly diagnosed MM. The [^{18}F]FPRGD$_2$ PET/CT images ((a) maximum intensity projection, MIP, and sagittal slices) show two spinal FLs with [^{18}F]FPRGD$_2$ uptake: one in the vertebral body of T5 corresponding to a mixed lesion on CT images ((a) red arrows) and a pathologic fracture of T8 ((a) green arrows). The [^{18}F]NaF/[^{18}F]FDG PET/CT images ((b) MIP and sagittal slices) show [^{18}F]NaF/[^{18}F]FDG uptake in T8 ((b) green arrows) but not in T5 ((b) red arrows). In addition, [^{18}F]FPRGD$_2$ uptake was also observed in glenohumeral, left hip, and right ankle joints ((a) blue arrows) as well as in the left total knee arthroplasty ((a) orange arrow). The observation of [^{18}F]FPRGD$_2$ uptake in musculoskeletal disorders has already been published [6].

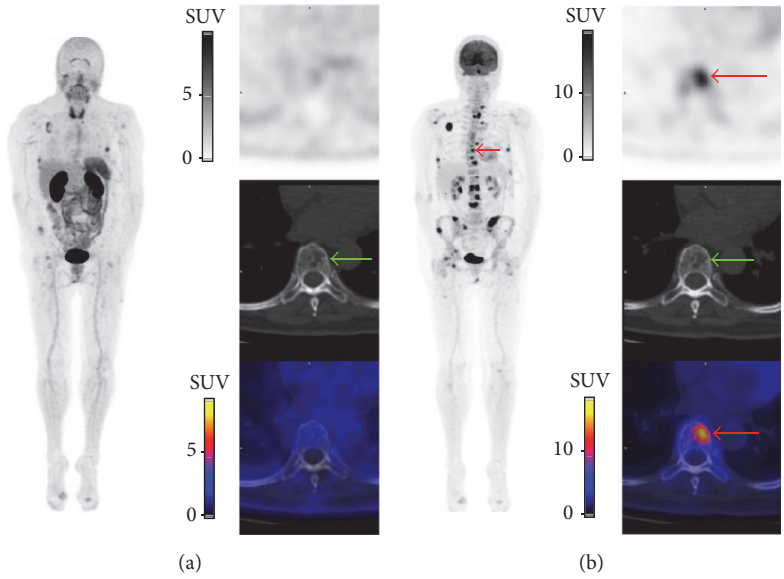

Figure 3: [^{18}F]FPRGD$_2$ PET/CT (a) and [^{18}F]NaF/[^{18}F]FDG PET/CT (b) images of patient #3 with MM at time of relapse, more than 4 years after diagnosis and end of treatment. The number of osteolytic FLs with [^{18}F]FPRGD$_2$ uptake (n = 28) was far lower than with [^{18}F]NaF/[^{18}F]FDG uptake (n = 40). The green arrows point at an osteolytic FL of T9 showing high [^{18}F]NaF/[^{18}F]FDG uptake ((b) red arrows; SUV$_{max}$ 10.2) but no focal [^{18}F]FPRGD$_2$ uptake ((a) SUV$_{max}$ 1.8).

tumor cell metabolism and/or bone formation. The heterogeneous uptake of [^{18}F]FPRGD$_2$ can be explained by biological phenomena and previously received treatments. The myeloma-induced angiogenesis appears after an "angiogenic switch" due to the release of angiogenic factors by subsets of myeloma cells or can be directly in proportion to the tumor infiltration inside the bone marrow [22]. This angiogenesis is counteracted by targeted treatments such as thalidomide and bortezomib which could explain reduced uptake in relapsing patients. Decreased uptake of [^{18}F]FDG was recently found to be associated with reduced expression of *hexokinase-2*, responsible for the first step of glycolysis [23].

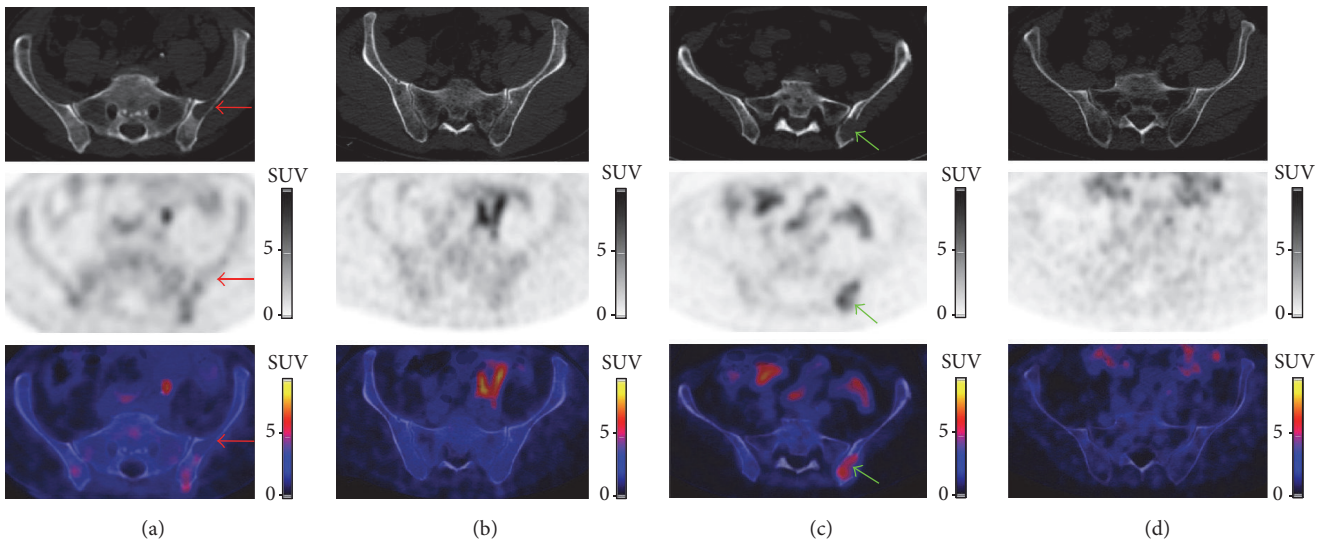

Figure 4: [^{18}F]FPRGD$_2$ PET/CT images of all patients. A diffuse bone marrow involvement was described based on CT images in patients #1 (a) and #2 (b); the [^{18}F]FPRGD$_2$ PET images also showed diffuse and heterogeneous bone marrow [^{18}F]FPRGD$_2$ uptake in patients #1 (a) and a mild diffuse bone marrow uptake in patient #2 (b). In contrast, no diffuse bone marrow [^{18}F]FPRGD$_2$ uptake was seen in patients #3 ((c) the green arrows point at a lytic FL with [^{18}F]FPRGD$_2$ uptake) and #4 ((d) no lesion shown). Note that, in patient #1 (a) with newly diagnosed MM, a large osteolytic FL in CT images did not show [^{18}F]FPRGD$_2$ uptake above the bone marrow background ((a) red arrows).

Table 3: Focal lesions detected per patient.

Patient	Newly diagnosed MM		Relapsed-MM		Total
	# 1	# 2	# 3	# 4	
Concordant results[†]	2	1	28	0	*31*
[^{18}F]FPRGD$_2$+ and [^{18}F]NaF/FDG−	5	0	0	0	*5*
[^{18}F]FPRGD$_2$− and [^{18}F]NaF/FDG+	3	0	12	1	*16*
[^{18}F]FPRGD$_2$ & CT− and [^{18}F]NaF/FDG+	0	0	1	0	*1*
CT− and [^{18}F]FPRGD$_2$+	0	0	0	0	*0*
CT+ and both PET−	8	2	10	0	*20*
Total malignant lesions	*18*	*3*	*51*	*1*	*73*
Fractures	3	3	1	1	8

[†]Osteolytic FLs showing both [^{18}F]FPRGD$_2$ and [^{18}F]NaF/FDG uptake.

Even though this case report suggests that [^{18}F]FPRGD$_2$ PET/CT might not be appropriate for detection of MM lesions, it may be of use in the assessment of integrin $\alpha_v\beta_3$ expression in MM lesions, especially in clinical trials evaluating inhibitors targeting $\alpha_v\beta_3$ integrins, as recently investigated by Tucci et al. [24]. In addition, our study focused on patients with symptomatic myeloma disease, while [^{18}F]FPRGD$_2$ PET/CT might be useful to detect bone marrow infiltration in precursor states of the disease (smoldering multiple myeloma or monoclonal gammopathy of undetermined significance).

5. Conclusions

In this case report, [^{18}F]FPRGD$_2$ PET/CT detected only 50% of the FLs detected by CT suggesting that the clinical utility of [^{18}F]FPRGD$_2$ PET/CT is rather limited for the detection of overt MM lesions. However, the clinical and possibly prognostic relevance of [^{18}F]FPRGD$_2$ positive MM lesions needs further investigation.

Abbreviations

PET: Positron emission tomography
CT: Computed tomography
[^{18}F]FDG: [^{18}F]Fluorodeoxyglucose
FL: Focal lesion
MM: Multiple myeloma
WB: Whole-body
IMWG: International Myeloma Working Group
SUV: Standardized uptake value
SD: Standard deviation.

Ethical Approval

All procedures performed in this report were in accordance with the ethical standards of the institutional research

committee and with the principles of the 1964 Declaration of Helsinki and its later amendments or comparable ethical standards. This Belgian monocentric prospective protocol (EudraCT 2013-004807-38) was approved by the Ethics Committee of the University Hospital of Liege and the Federal Agency for Medicines and Health Products (FAMHP).

Consent

Every enrolled patient signed specific informed consent.

Conflicts of Interest

The authors declare that they have no conflicts of interest.

Authors' Contributions

Nadia Withofs and Roland Hustinx supervised PET/CT image acquisition and analyzed the PET/CT images. François Cousin analyzed the CT images. Sanjiv S. Gambhir shared his expertise in [^{18}F]FPRGD$_2$ PET/CT. Jo Caers and Yves Beguin designed the study and recruited and informed patients. Bernard De Prijck and Christophe Bonnet informed and recruited patients. Every author contributed to the writing of the manuscript.

Acknowledgments

The authors thank Frederic Mievis, Fabrice Giacomelli, and Christine Mella (Cyclotron Research Centre, University of Liege, Belgium) for the syntheses of [^{18}F]FPRGD$_2$ and [^{18}F]NaF. This work has been supported by grants from the Foundation against Cancer, Fonds de la Recherche Scientifique Médicale, FIRS Research Fund (CHU de Liège), the Fonds National de la Recherche Scientifique (FNRS, Belgium), and the Fonds Spéciaux de la Recherche (University of Liege).

References

[1] S. V. Rajkumar, M. A. Dimopoulos, and A. Palumbo, "International Myeloma Working Group updated criteria for the diagnosis of multiple myeloma," *The Lancet Oncology*, vol. 15, no. 12, pp. e538–e548, 2014.

[2] J. Caers, C. F. De Larrea, X. Leleu et al., "The changing landscape of smoldering multiple myeloma: a european perspective," *Oncologist*, vol. 21, no. 3, pp. 333–342, 2016.

[3] M. Cavo, E. Terpos, C. Nanni et al., "Role of ^{18}F-FDG PET/CT in the diagnosis and management of multiple myeloma and other plasma cell disorders: a consensus statement by the International Myeloma Working Group," *The Lancet Oncology*, vol. 18, no. 4, pp. e206–e217, 2017.

[4] Z. Wu, Z.-B. Li, W. Cai et al., "^{18}F-labeled mini-PEG spacered RGD dimer (^{18}F-FPRGD$_2$): synthesis and microPET imaging of $\alpha_v\beta_3$ integrin expression," *European Journal of Nuclear Medicine and Molecular Imaging*, vol. 34, no. 11, pp. 1823–1831, 2007.

[5] D. Thonon, D. Goblet, E. Goukens et al., "Fully automated preparation and conjugation of N-succinimidyl 4-[^{18}F]fluorobenzoate ([^{18}F]SFB) with RGD peptide using a GE FASTlab synthesizer," *Molecular Imaging and Biology*, vol. 13, no. 6, pp. 1088–1095, 2011.

[6] N. Withofs, E. Charlier, P. Simoni et al., "^{18}F-FPRGD$_2$ PET/CT imaging of musculoskeletal disorders," *Annals of Nuclear Medicine*, vol. 29, no. 10, pp. 839–847, 2015.

[7] N. Withofs, N. Signolle, J. Somja et al., " ^{18}F-FPRGD$_2$ PET/CT imaging of integrin $\alpha_v\beta_3$ in renal carcinomas: correlation with histopathology," *Journal of Nuclear Medicine*, vol. 56, no. 3, pp. 361–364, 2015.

[8] N. Withofs, P. Martinive, J. Vanderick et al., "[^{18}F]FPRGD$_2$ PET/CT imaging of integrin $\alpha_v\beta_3$ levels in patients with locally advanced rectal carcinoma," *European Journal of Nuclear Medicine and Molecular Imaging*, vol. 43, no. 4, pp. 654–662, 2016.

[9] R. Haubner, HJ. Wester, U. Reuning, R. Senekowitsch-Schmidtke, B. Diefenbach, and H. Kessler, "Radiolabeled $\alpha_v\beta_3$ integrin antagonists: a new class of tracers for tumor targeting," *Journal of Nuclear Medicine*, pp. 40–1061, 1999.

[10] S. M. Weis and D. A. Cheresh, "α_v integrins in angiogenesis and cancer," *Cold Spring Harbor perspectives in medicine*, vol. 1, no. 1, p. a006478, 2011.

[11] F. C. Gaertner, H. Kessler, H.-J. Wester, M. Schwaiger, and A. J. Beer, "Radiolabelled RGD peptides for imaging and therapy," *European Journal of Nuclear Medicine and Molecular Imaging*, vol. 39, no. 1, pp. S126–S138, 2012.

[12] L. Seguin, J. S. Desgrosellier, S. M. Weis, and D. A. Cheresh, "Integrins and cancer: regulators of cancer stemness, metastasis, and drug resistance," *Trends in Cell Biology*, vol. 25, no. 4, pp. 234–240, 2015.

[13] T. J. Wadas, H. Deng, J. E. Sprague, A. Zheleznyak, K. N. Weilbaecher, and C. J. Anderson, "Targeting the $\alpha_v\beta_3$ integrin for small-animal PET/CT of osteolytic bone metastases," *Journal of Nuclear Medicine*, vol. 50, no. 11, pp. 1873–1880, 2009.

[14] K. Cohen, N. Flint, S. Shalev et al., "Thyroid hormone regulates adhesion, migration and matrix metalloproteinase 9 activity via $\alpha_v\beta_3$ integrin in myeloma cells," *Oncotarget*, vol. 5, no. 15, pp. 6312–6322, 2014.

[15] S. Stucci, M. Tucci, A. Passarelli, and F. Silvestris, "$\alpha_v\beta_3$ integrin: Pathogenetic role in osteotropic tumors," *Critical Reviews in Oncology/Hematology*, vol. 96, no. 1, pp. 183–193, 2015.

[16] J. G. Schneider, S. R. Amend, and K. N. Weilbaecher, "Integrins and bone metastasis: Integrating tumor cell and stromal cell interactions," *Bone*, vol. 48, no. 1, pp. 54–65, 2011.

[17] J. Caers, U. Günthert, H. De Raeve et al., "The involvement of osteopontin and its receptors in multiple myeloma cell survival, migration and invasion in the murine 5T33MM model," *British Journal of Haematology*, vol. 132, no. 4, pp. 469–477, 2006.

[18] A. Iagaru, E. Mittra, S. S. Yaghoubi et al., "Novel strategy for a cocktail ^{18}F-fluoride and ^{18}F-FDG PET/CT scan for evaluation of malignancy: results of the pilot-phase study," *Journal of Nuclear Medicine*, vol. 50, no. 4, pp. 501–505, 2009.

[19] S. C. Sampath, S. C. Sampath, C. Mosci et al., "Detection of osseous metastasis by ^{18}F-NaF/^{18}F-FDG PET/CT versus CT alone," *Clinical Nuclear Medicine*, vol. 40, no. 3, pp. e173–e177, 2015.

[20] N. Withofs, F. Cousin, T. Tancredi, Simoni P., De Prijck B., Hafraoui K. et al., "Comparison of combined whole-body [^{18}F]NaF and [^{18}F]FDG PET/CT versus MRI for the detection of myeloma lesions," *Journal of Nuclear Medicine*, vol. 57, supplement 2, article 606, 2016.

[21] C. Sachpekidis, J. Hillengass, H. Goldschmidt et al., "Treatment response evaluation with ^{18}F-FDG PET/CT and ^{18}F-NaF PET/CT in multiple myeloma patients undergoing high-dose chemotherapy and autologous stem cell transplantation," *European Journal of Nuclear Medicine and Molecular Imaging*, vol. 44, no. 1, pp. 50–62, 2017.

[22] E. Otjacques, M. Binsfeld, A. Noel, Y. Beguin, D. Cataldo, and J. Caers, "Biological aspects of angiogenesis in multiple myeloma," *International Journal of Hematology*, vol. 94, no. 6, pp. 505–518, 2011.

[23] L. Rasche, E. Angtuaco, J. E. McDonald et al., "Low expression of hexokinase-2 is associated with false-negative FDG–positron emission tomography in multiple myeloma," *Blood*, vol. 130, no. 1, pp. 30–34, 2017.

[24] M. Tucci, S. Stucci, C. Felici et al., "Cilengitide restrains the osteoclast-like bone resorbing activity of myeloma plasma cells," *British Journal of Haematology*, vol. 173, no. 1, pp. 59–69, 2016.